National Aeronautics and Space Administration

Orbital Debris Quarterly News

Volume 13, Issue 1

January 2009

Inside...

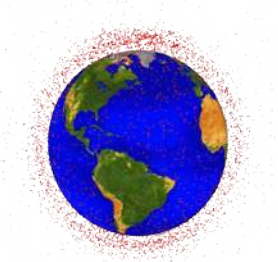

A publication of

The NASA Orbital Debris Program Office

New Debris Seen from Decommissioned Satellite with Nuclear Power Source

A 21-year-old satellite containing a dormant nuclear reactor was the source of an unexpected debris cloud in early July 2008. Launched by the former Soviet Union in February 1987, Cosmos 1818 (International Designator 1987-011A, U.S. Satellite Number 17369) was the first of two vehicles designed to test a new, more advanced nuclear power supply in low Earth orbit. Dozens of small particles were released during the still-unexplained debris generation event.

Cosmos 1818 and its sister spacecraft, Cosmos 1867 (Figure 1), carried a thermionic nuclear power supply, in contrast to the simpler, thermoelectric nuclear device which provided energy to the well-known RORSATs (Radar Ocean Reconnaissance Satellites) during the 1970s and 1980s. The most infamous RORSAT was Cosmos 954, which rained radioactive debris over Canada in 1978 after suffering a loss of control malfunction. According to Russian reports, the nuclear reactors on Cosmos 1818 and Cosmos 1867 functioned for approximately 6 and 12 months, respectively. For the next two decades, the two inactive spacecraft circled the Earth without significant incident.

Following the fragmentation event on or about 4 July 2008, the U.S. Space Surveillance Network was able to produce orbital data on 30 small debris (Figure 2). The majority of these debris were ejected in a posigrade direction with velocities of less than 15 meters per second, suggesting a relatively low energy event. From radar detections, a larger number of very small debris appear to have also been released, but routine tracking of these debris has proven difficult.

Special observations of a few of the debris revealed characteristics generally indicative of metallic spheres. Cosmos 1818 employed sodium-potassium (NaK) as a coolant for its reactor, as did

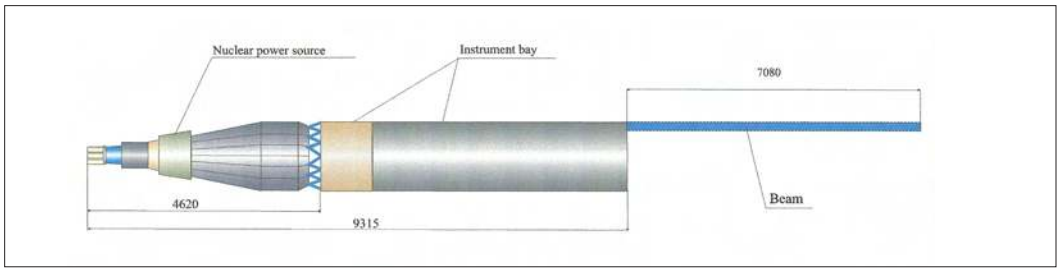

Figure 1. Simplified illustration of Cosmos 1818 and Cosmos 1867. The dimensional units are millimeters.

Unlike their RORSAT cousins, which operated in very low orbits near 250 km, Cosmos 1818 and Cosmos 1867 were directly inserted into orbits near 800 km, eliminating any threat of premature reentry. the older RORSATs. Although the post-Cosmos 954 RORSATs were known for releasing significant amounts of NaK droplets after reaching their

continued on page 2

New Debris

continued from page 1

disposal orbits (Kessler *et al.*, 1997), Cosmos 1818 and Cosmos 1867 did not follow this precedent.

Much of the NaK within Cosmos 1818 probably was in a solid state at the time of the debris generation event. However, some NaK present in the radiator coolant tubes might have reached a temporary liquid state, particularly when the spacecraft was exposed to direct solar illumination. A breach in a coolant tube (for example, due to long-term thermal stress) at such a time could have resulted in the release of NaK droplets. Further, the hypervelocity impact of a small particle might have generated sufficient heat to melt some of the NaK, which then would have formed spheres with metallic properties. Additional analysis of the debris is underway in hopes of providing new insights into the nature of the objects and the possible cause of their origin. To date, no similar debris generation by Cosmos 1867 has been observed.

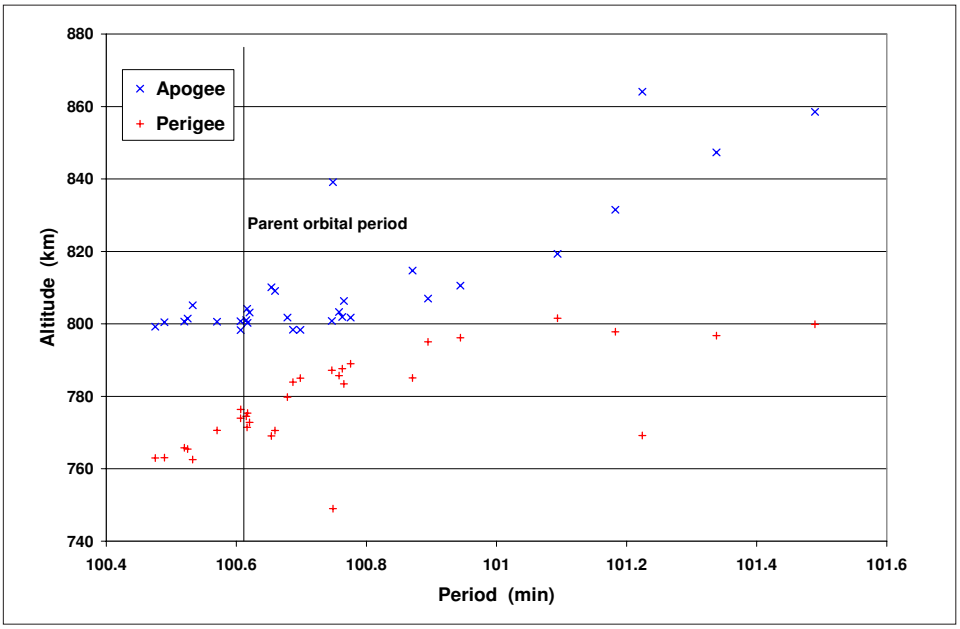

Figure 2. Distribution of 30 tracked debris from Cosmos 1818.

1. Kessler, D.J., *et al.*, The Search for a Previously Unknown Source of Orbital Debris: The Possibility of a Coolant Leak in Radar Ocean Reconnaissance Satellites, JSC-27737, NASA Johnson Space Center, 21 February 1997. ♦

Fengyun-1C Debris: Two Years Later

Two years after the destruction of the Fengyun-1C meteorological satellite by a Chinese anti-satellite (ASAT) interceptor, the resultant debris cloud remains pervasive throughout low Earth orbit (LEO), accounting for more than 25% of all cataloged objects there. A total of 2378 fragments greater than 5 cm in diameter have been officially cataloged by the U.S. Space Surveillance Network from the one-metric-ton vehicle (Figure 1), and more than 400 additional debris are being tracked but have not yet been cataloged. The estimated population of debris larger than 1 cm is greater than 150,000.

Figure 2 indicates that the Fengyun-1C debris cloud, which poses collision risks to all operational spacecraft in LEO and in elliptical orbits passing through LEO, now completely envelopes the Earth. Since their creation on 11 January 2007, less than 2% of the cataloged debris have fallen back to Earth. Many of the debris will stay in orbit for decades, and some for more than a century.

The Fengyun-1C debris cloud easily constitutes the largest collection of fragments in Earth orbit. By comparison, the second-greatest population of cataloged debris still in orbit originated from the former Soviet Cosmos 1275 navigation satellite, which suffered a battery explosion in 1981 and is only one-tenth as numerous as the Fengyun-1C debris cloud. ♦

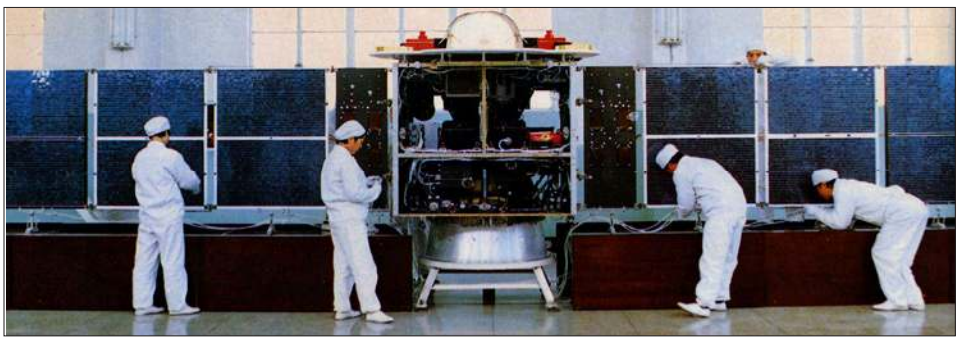

Figure 1. A Fengyun-1 class satellite in final integration.

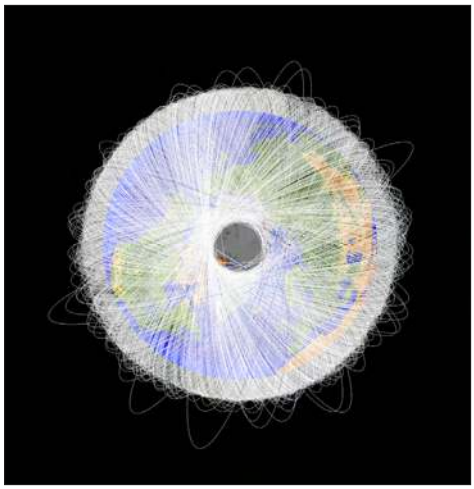

Figure 2. Orbital paths of nearly 2800 tracked orbital debris from the Fengyun-1C satellite 2 years after its destruction in a Chinese ASAT test.

PROJECT REVIEWS

Quantitative Analysis of the European Space Agency's Automated Transfer Vehicle "Jules Verne" Reentry Event of 29 September 2008

E. BARKER, M. MULROONEY, AND P. MALEY

The Orbital Debris Program Office (ODPO) at NASA-JSC was selected to participate in the data acquisition and analysis effort associated with the recent 29 September reentry and break-up of the European Space Agency's (ESA) Automated Transfer Vehicle "Jules Verne" (ATV-1; Figure 1). This is the first of a series of vehicles developed

Figure 1. "Jules Verne" Automated Transfer Vehicle (ESA Graphic).

to service the International Space Station (ISS) as a disposable re-supply, re-boost, and refuse spacecraft. ATV's automated, crewless operation makes it a cost effective and efficient means to deliver supplies, act as a depository for waste, and provide orbital reboosts to the ISS on an approximately annual timeline. At end-of-mission, the ATV separates from the ISS, performs a de-orbit burn, and undergoes a destructive reentry in the Earth's atmosphere.

The final moments of ATV-1 "Jules Verne" were observed in detail by a joint ESA-NASA Multi-instrument Aircraft Campaign (JV-MAC). Details of the campaign are available at <http://atv.seti.org/>. The spacecraft's reentry was observed with a range of instruments to determine how the ATV breaks up as it passes through the Earth's atmosphere. Providing valuable information to compare with previously developed computer models of the ATV reentry, the analysis will help enhance public risk assessments of future reentries of the ATV and other ESA and NASA spacecraft. Of particular interest was the time and altitude of the primary fuel tank disruption. To further this effort, NASA-JSC/ODPO agreed to engage in data acquisition of the break-up and subsequent photometric and trajectory analysis of the multitude of fragments separating and streaming from the vehicle. An imaging system developed by Paul D. Maley of United Space Alliance at NASA-JSC, was utilized for data acquisition. As lead of the ODPO Optical Measurements Group, Dr. Edwin Barker (Figure 2) was selected to operate the imaging system, which consisted of 75 mm and 12 mm objective lenses, each one connected to a third-generation microchannel plate intensifier; each lens/intensifer system fed images in the 4000-8000 Angstrom range into a commercial, low-light, off-the-shelf security camera (PC-164 and Watec 902H). Data from both systems were recorded on Hi-8 format digital camcorders. The cameras were co-aligned and yielded simultaneous wide (~20 degrees) and narrow (~8 degrees) field views of the break-up event. Having two cameras enabled views of fragments close to the parent target, as well as a larger scale assessment of the debris trail. Dual cameras also provided some redundancy in the event of a single failure. The narrow field camera was primarily aimed behind the bright portion of the reentry fireball in order to avoid saturation.

The JV-MAC campaign was performed entirely from two aircraft commissioned by ESA and the science team was coordinated by Dr. Peter Jenniskens of the SETI Institute.

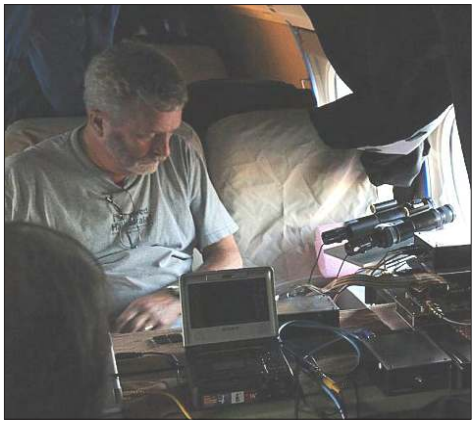

Figure 2. Dr. Barker aboard the Gulfstream V with the dual low-light cameras positioned at the aircraft window. (Credit: Bryan Murahashi 2008).

Airborne measurements were required to ensure timely access to the unpopulated geographical location, where the reentry could be observed in the Southern Pacific Ocean, south of Tahiti (see Figure 3). A NASA DC-8 was positioned near the end of the reentry path and the Gulfstream V (provided for this effort by Google Corporation) was positioned upstream at a point where the major disruption was predicted to occur.

continued on page 4

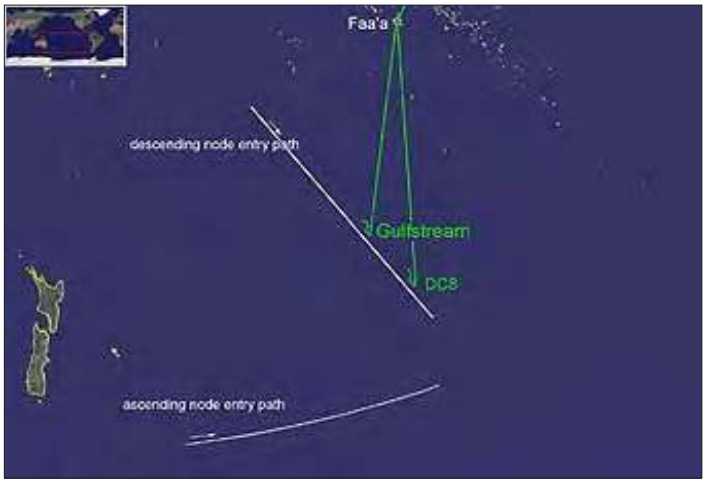

Figure 3. Reentry path of ATV-1 (schematic) and the positioning of the two aircraft in the ATV-1 "Jules Verne" Multi-Instrument Aircraft Campaign (ESA Graphic).

Reentry Event

continued from page 3

Figure 4. Gulfstream V observing team (Credit: Bryan Murahashi 2008).

Figure 5. Video still image of ATV-1 and 3 reflections due to aircraft window.

The Gulfstream V jet provided a platform that could turn to follow the ATV-1 as it moved across the sky. The JV-MAC aircraft supported several different instrument packages including wide/narrow field and intensified cameras, imaging spectrographs, high frame-rate cameras, and HDTV cameras. The NASA DC-8 carried 13 experiments and the Gulfstream V carried 6 experiment packages with several duplicate setups to protect against the failure of any single instrument. Instrument teams were composed of researchers from several ESA and NASA centers, universities, and other institutions. The Barker/Maley instruments (JSCINT) were assigned to a window in the Gulfstream V. Two high-speed cameras, a low-light spectrometer, a near infrared camera, and an HDTV camera were assigned to other windows in the Gulfstream V (Gulfstream experimenters are shown in Figure 4). While several CCD video cameras recorded the reentry, the JSCINT system was one of two intensified systems whose goal was to image the fainter debris targets. Accurate timing and aircraft location was provided by distributed GPS systems on both aircraft.

The ATV-1 reentry event was visible from the aircraft for approximately 4 minutes and its trajectory and arrival time were very close to those predicted. Barker successfully acquired the target (Figure 5 shows the image of ATV-1 and three reflections from the aircraft window) some seconds after it rose above the horizon and followed as it traversed the sky at a peak rate of about 3 degrees per second. The video data, although saturated in the immediate vicinity of the parent target due to its extreme brightness, is of sufficient quality to differentiate many of the fragments as they emerge from the saturated zone a few degrees aft along the trail.

The ODPO was assigned the assessment of the relative motions and brightness of the fainter trailing debris fragments as its primary scientific objective. The

continued on page 5

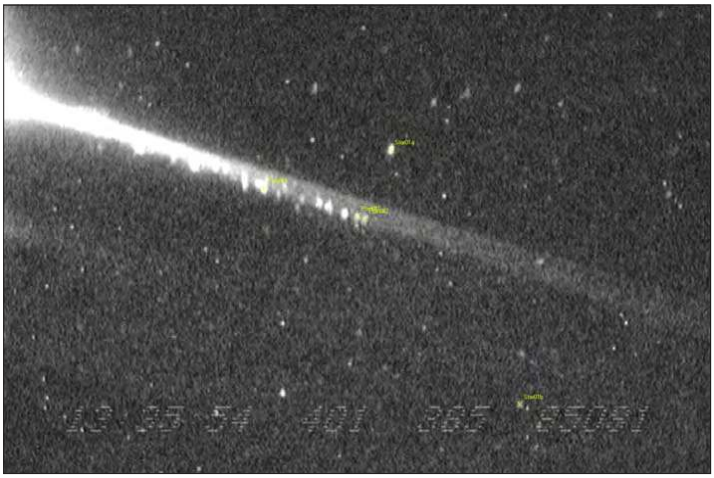

Figure 6. Identification of reference stars and debris fragments using TrackEye software.

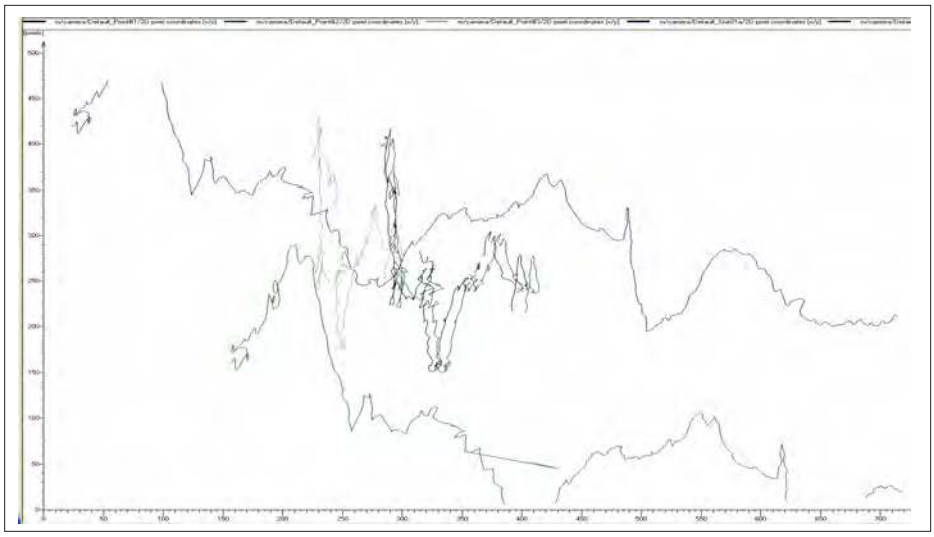

Figure 7. Raw two-dimensional positional information from a 10-second video sequence. The abscissa and ordinate are the x and y star (2) and target (3) positions in the video sequence. (Approximately 300 frames are represented here).

Reentry Event

continued from page 4

resultant relationship between brightness and drift rate will be analyzed for what it might indicate about the action of atmospheric drag on these fragments. Additionally, brightness variations for a given fragment will be assessed, as they may loosely correlate with area-to-mass ratio and, thereby, also with drift rate.

Quantitative analysis of the video consists of two parts – coordinate transformation and photometry. The former requires identification of field stars to use as references points with known celestial coordinates (Right Ascension and Declination). Since the aircraft, observer, and target are all moving, both rotational and lateral motion must be transformed. A program called TrackEye, developed by Photosonics, Inc. for target tracking, has been employed to assist in this regard. Selecting target fragments and reference stars within TrackEye (Figure 6) enables a frame-by-frame track and coordinate transformation for each discrete fragment detectable above the noise threshold. Although frequent user intervention is required to follow the fainter targets (approximately 7th magnitude), TrackEye does simplify the process by generating an output file with absolute and relative target coordinates that can be transformed to individual target trajectories. Figure 7 shows the raw two-dimensional positional information from a 10-second video sequence; it clearly shows the erratic camera motion of two reference stars (heavy lines) and three tracked fragments.

Figure 8, comparing pixel separation versus time, shows the same sequence with the coordinate transformation applied. The star positions are now constant in time, and the motion of the fragments with respect to them is changing.

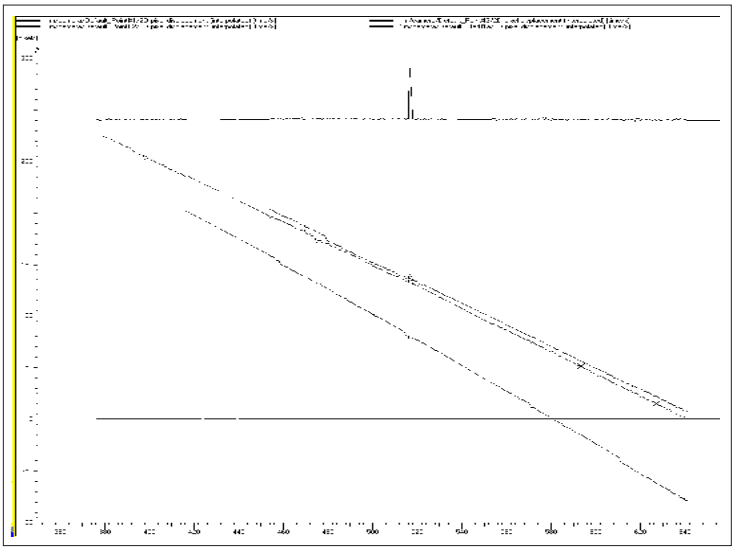

Figure 8. Same sequence as Figure 7, but with the coordinate transform applied. The abscissa is now the time axis and the ordinate is defined by the two reference stars. The target positions are plotted as time dependent displacements along the line adjoining the reference stars. (Approximately 300 frames are represented here).

The photometric portion of the analysis uses these same stars to logarithmically calibrate the video intensity values. Targets are then measured manually in programs such as IRAF or ImageJ.

The ATV-1 reentry presents a unique opportunity to study the dynamical evolution of an atmospheric fragmentation event. NASA diligently acquired over 5000 frames of video data with as many as 60 fragmentation targets per frame. As such, this represents a challenging, but potentially rewarding, analysis effort. When the analysis is completed we plan to present them in a future ODQN article. ♦

Two New Microsatellite Impact Tests in 2008

J. MURAKAMI, T. HANADA, J.-C. LIOU, AND E. STANSBERY

In an effort to continue the investigation of the physical properties of breakup fragments originating from satellites made of modern materials and fragments of multi-layer insulation (MLI) and solar panels, two additional impact tests were conducted in 2008. The effort is part of an on-going collaboration between Kyushu University in Japan and the NASA Orbital Debris Program Office. This article provides a preliminary summary of the two tests.

The target satellites prepared for the tests were similar to those used in the previous experiments.[1] The main structure of each microsatellite was composed of five layers (top and bottom layers and three internal layers) and four side panels. They were assembled with angle bars made of aluminum alloy and metal spacers. The top and bottom layers and the four side panels were made of Carbon Fiber Reinforced Plastics (CFRP) while the three inner layers were made of Glass Fiber Reinforced Plastics (GFRP). In addition, the interior of each microsatellite was equipped with fully functional electronic devices, including a wireless radio; nickel-hydrogen batteries; and communication, power supply, and command/data handling circuits. New materials added to the two satellites were MLI and solar panels: (1) the four side panels and the bottom layer were covered with MLI, and (2) a solar panel was attached to one of the side panels. The solar panel had six solar cells on an aluminum honeycomb sandwich panel with CFRP face sheets. The MLI consists of two sections, A and B, as shown in Figure 1. Section A covered the

continued on page 6

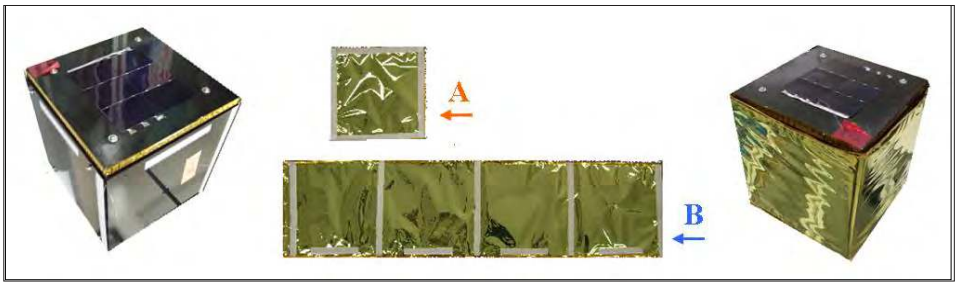

Figure 1. Target microsatellites and MLIs; (left) target microsatellite not covered with MLI, (center) MLIs, (right) target microsatellite covered with MLI. A solar panel consists of six solar cells and an aluminum honeycomb sandwich panel with CFRP face sheets.

Impact Tests

continued from page 5

bottom layer while section B covered the four side panels. MLI sections were attached to the satellite surfaces with Velcro. The dimensions of the satellites were identical to those used in the previous tests, 20 cm x 20 cm x 20 cm. Due to the addition of MLI and solar panels, the total mass of each satellite was approximately 1500 grams, slightly higher than the previous

continued on page 7

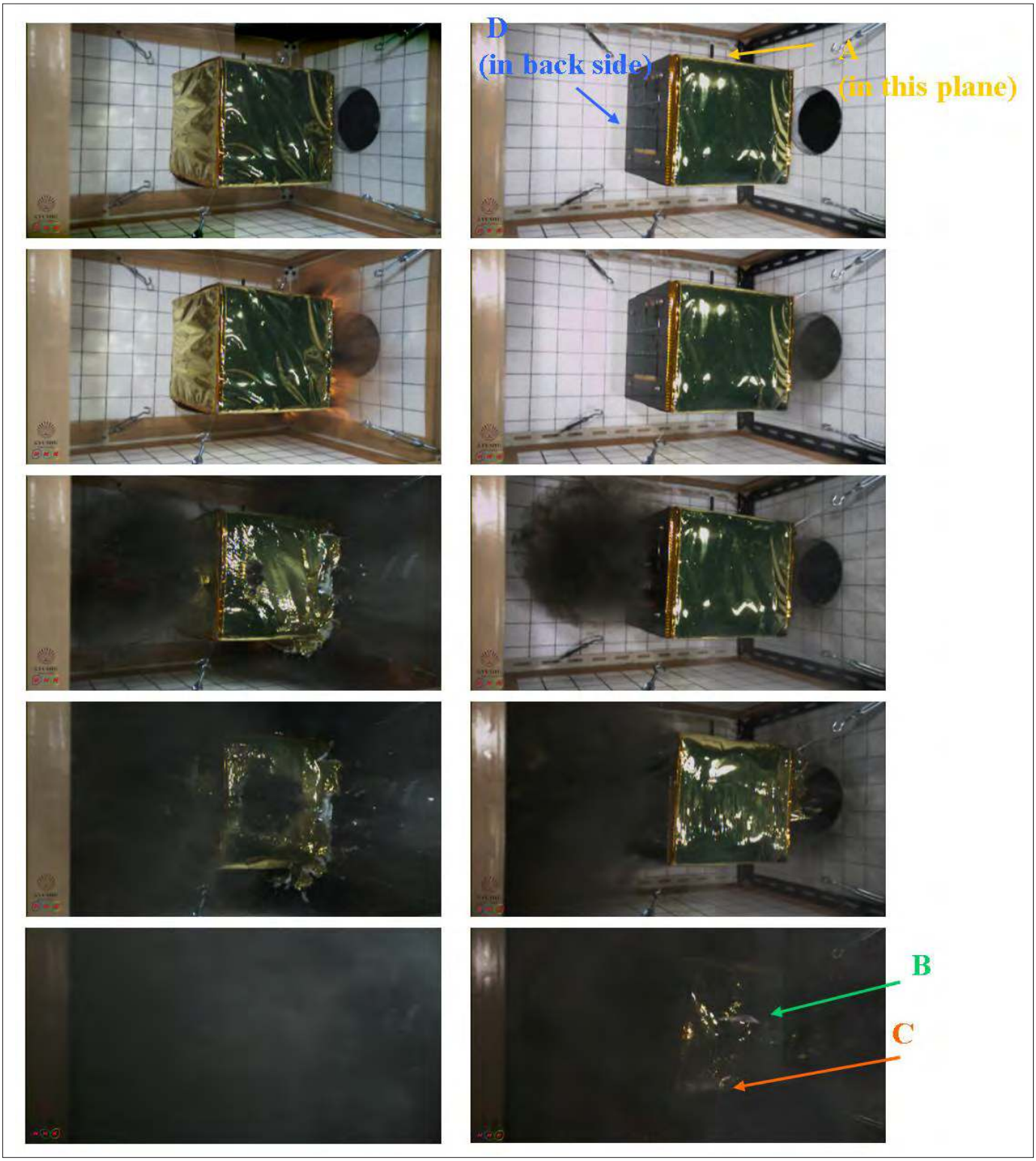

Figure 2. Impact fragmentation; (left) Shot F, (right) Shot R. The locations of MLI tearing were captured in Shot R. (See point A to D, also in Fig.4.)

Impact Tests

continued from page 6

targets (1300 grams).

The impact tests were carried out using the two-stage light gas gun at Kyushu Institute of Technology in Kitakyushu, Japan. To indicate the locations of the solar panels with respect to the incoming projectiles, the two shots were labeled "F" and "R" (see also Figure 5). The impact speeds of Shot F and Shot R were 1.74 km/s and 1.78 km/s, respectively, and the ratio of impact kinetic energy to the target mass for the two tests was about 40 J/g. Both target satellites were completely fragmented after impact.

The impact fragmentations were captured by an ultra-high speed camera, in collaboration with the Japan Broadcasting Corporation (NHK in Japanese abbreviation). As shown in Figure 2, the impact fragmentations were recorded from two directions: edge-on and diagonally backward.

Figures 3 and 4 show large fragments and MLI pieces collected after the tests. There are noticeable differences between the two. Shot F generated more fragments and MLI pieces than Shot R. Regarding MLI pieces, a significant difference in size and number can be observed from Figure 4. The largest MLI piece in Shot F is similar in size to the CFRP layers or side panels, whereas in Shot R larger MLI pieces were preserved. As shown in Figures 2 and 4, the NHK's ultra-high speed camera clearly captured where the wraparound MLI was torn in Shot R. The number of needle-like fragments, broken up from the CFRP components, is also different between the two tests. Fragments from the impact plane and the back plane of the two tests are shown in Figure 5.

At least 1,500 or more fragments and 150 or more MLI pieces varying in size to a minimum of 2 mm are expected to be collected from Shot F. On the other hand, fewer fragments and MLI pieces are expected to be collected from Shot R. Once the collection is completed, fragments and MLI pieces will be measured and analyzed using the same method described in the NASA Standard Breakup Model.[2] Details of the new tests and preliminary results will be presented at the Fifth European Conference on Space Debris in 2009.

Figure 3. Fragments overview; (left) Shot F, (right) Shot R.

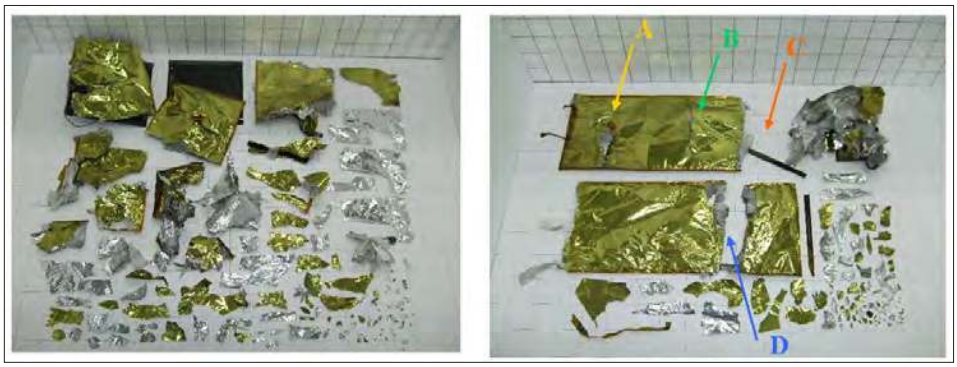

Figure 4. All MLI pieces collected; (left) Shot F, (right) Shot R.

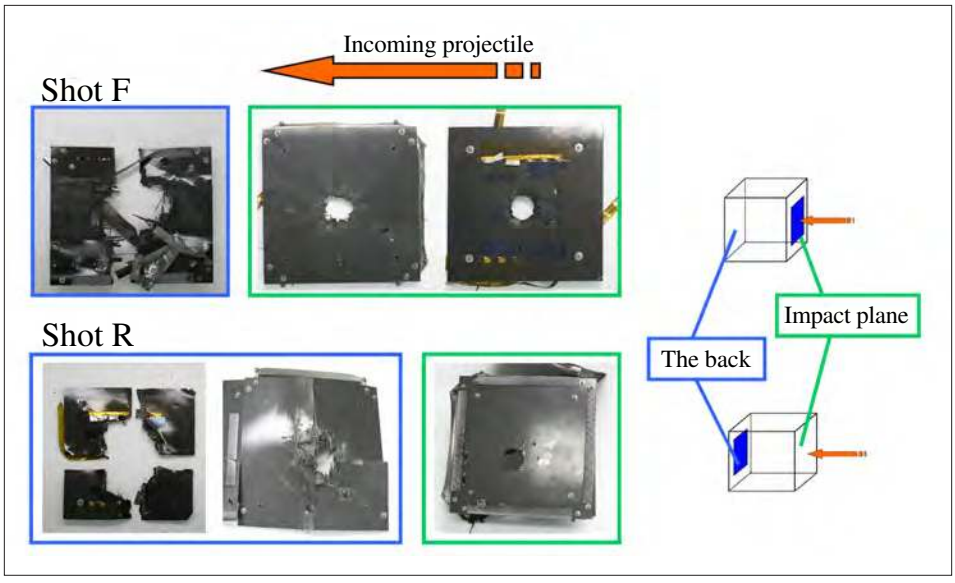

Figure 5. Impact plane and the back plane. The locations of the solar panels are shown in blue.

1. Hanada, T., Sakuraba, K., and Liou J.-C., Three New Satellite Impact Tests, Orbital Debris Quarterly News, Vol 11, Issue 4, 4-6, 2007.

2. Johnson, N. L., Krisko, P. H., Liou, J.-C., and Anz-Meador, P. D., NASA's New Breakup Model of EVOLVE 4.0, *Adv. Space Res.*, Vol. 28, No. 9, pp.1377-1384, 2001. ♦

A Review of Different Solar Cycle 24 Predictions and Other Long-Term Projections

D. WHITLOCK

There have been differing opinions on the potential magnitude of the upcoming 11-year solar cycle (#24). This cycle appears to have begun in the past few months as a handful of sunspots have been detected, indicating increasing solar activity. However, the lack of significant sunspot activity to date, as well as other measured solar characteristics, are leading forecasters to expect a potentially lower-than-usual cycle peak, and it may be the lowest seen in half a century.

Solar flux drives the altitude-independent, temporal variations in atmospheric density, which directly affect the decay rates of all objects in low Earth orbit (LEO). These unpredictable variations in density contribute to inevitable inaccuracies when models forecast the orbital lifetime of objects in this orbit regime. While historic solar flux values measured during periods of low solar activity show only slight variance from modeled values, solar flux activity measurements during high solar activity vary as much as 50% from the predictive models. The period of the solar cycle is not a constant either, and varies between cycles, such that the 11-year duration of the cycle is itself only an approximation.

The NASA Orbital Debris Program Office uses its Prop3D software tool for orbital lifetime prediction and for long-term orbital debris evolutionary models such as LEGEND (LEO-to-GEO Environment Debris model). A table of daily flux values is needed as a primary input into Prop3D to assist in lifetime estimations. The solar flux table used by Prop3D combines historical measured daily flux values (1957 – present), short term flux forecasts (present to 2015), and predicted future flux values based upon the historic measurement data. The historic daily measured flux and short term flux forecasts are made available by the National Oceanic Atmospheric Administration, Space Environmental Center (NOAA/SEC). For epochs beyond the near term (2016 and beyond), a curve-fit technique using sixth order sine and cosine terms was performed to fit historical daily solar flux values from 1947 through the current date; then this curve-fit equation is used to

continued on page 9

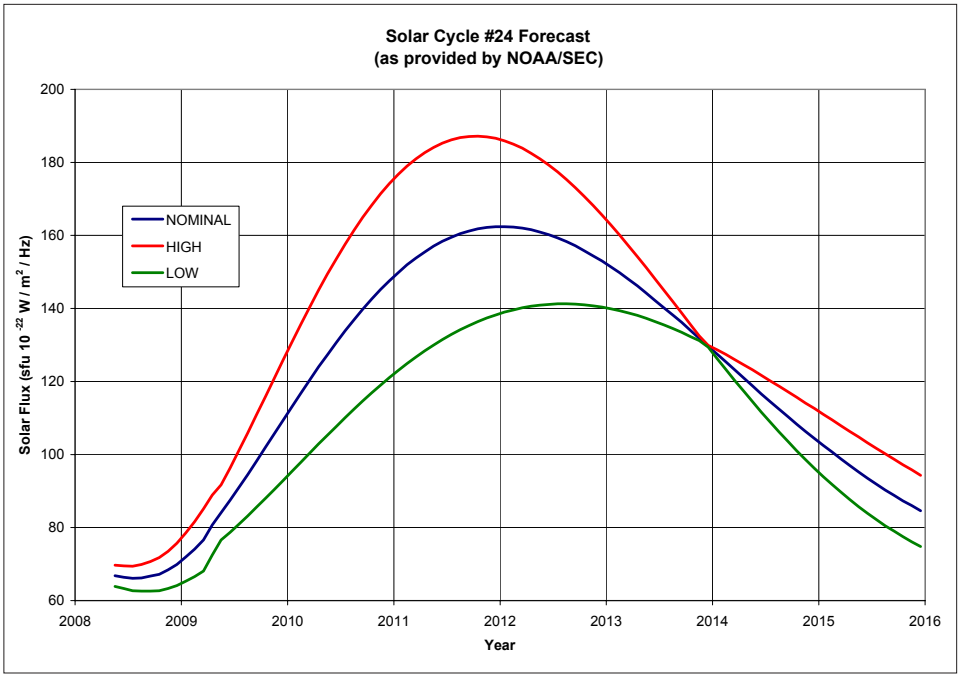

Figure 1. A comparison of the high, nominal, and low solar cycle #24 flux forecasts published in November 2008 by the National Oceanic and Atmospheric Administration, Space Environment Center (NOAA/SEC).

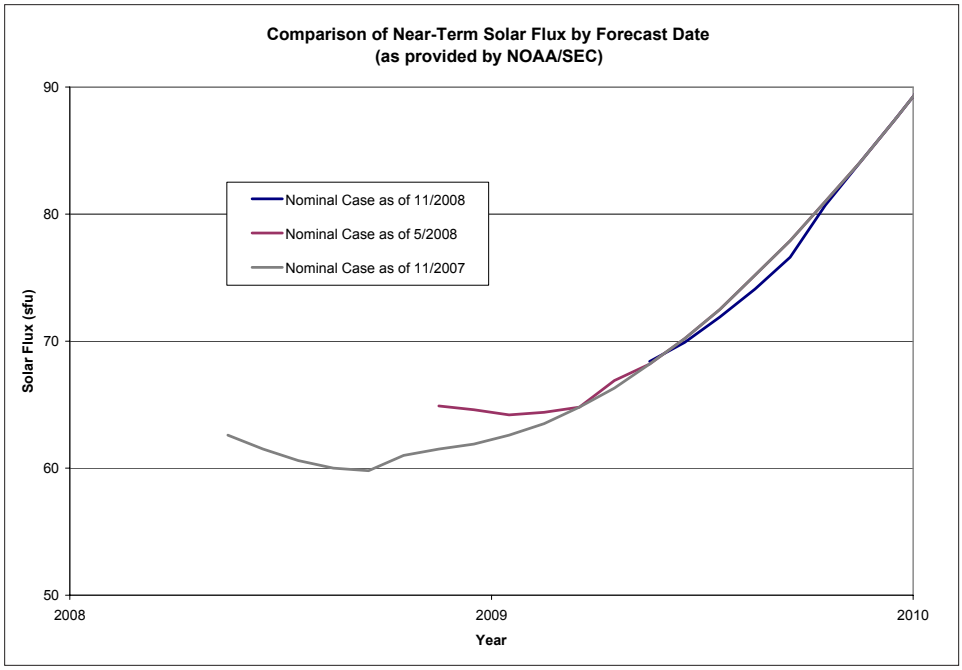

Figure 2. A comparison of the early portion of solar cycle #24 flux forcasts as functions of the date of the forecast.

Solar Cycle

continued from page 8-

generate future flux predicted values. The fitting technique (ODQN, April 2006, pp. 4-5) simultaneously determines 14 coefficients. The solar flux table is updated two times a year (May and November) to update the most recent 6 months of daily flux measurements and make very slight adjustments to future predictions. This table is included in the Debris Assessment Software package (DAS 2.0) for projects to use in order to estimate orbital lifetimes.

Figure 1 shows the current NOAA/SEC monthly forecast for Cycle #24, including "nominal", "high", and "low" cases. For the solar flux table used with Prop3D and DAS 2.0, the nominal case is used. This forecast is updated periodically, but since November 2007, only very small changes have been seen in the monthly forecast values in the nearer timeframes (*i.e.,* before 2010), as seen in Figure 2.

To demonstrate how the forecasted magnitude of the next cycle is atypically low, Figure 3 shows the Nominal NOAA/SEC forecast superimposed with the curve-fit of previous cycles. Also for comparison purposes, the monthly flux values of cycle #23 (moved to a corresponding epoch of cycle #24) are included in the figure to demonstrate how monthly values of a typical cycle would compare. Only seven monthly values for the last cycle (out of 90+ active months) would have been below the current forecast. Because of these low anticipated flux values, it is expected that resident objects with perigee altitude below about 1000 km will see appreciably longer lifetimes over the next decade or two, should the NOAA/SEC forecast come to fruition.

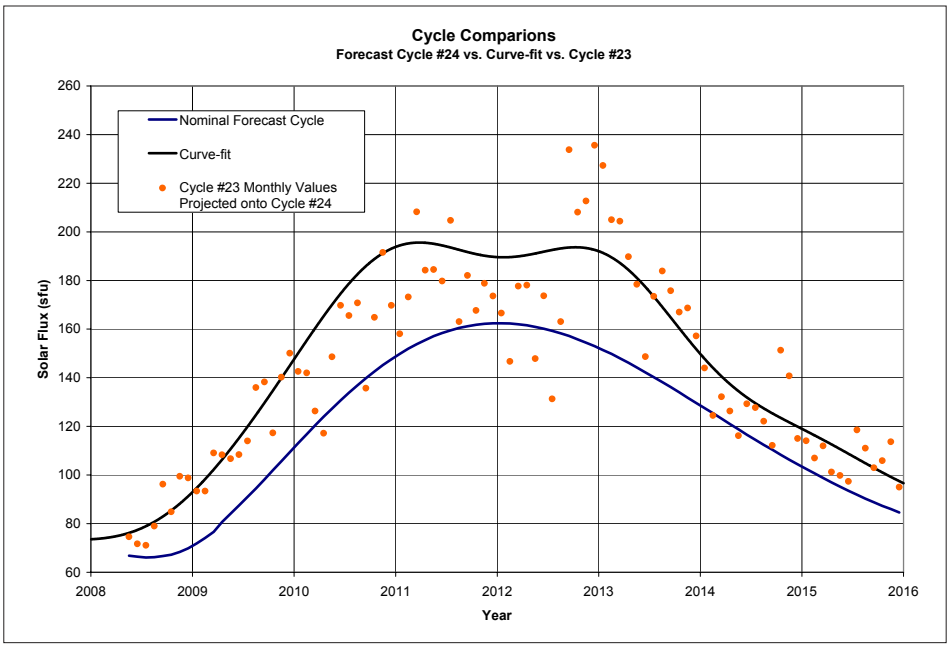

Figure 3. A comparison of the NOAA/SEC solar cycle #24 nominal flux forecast with a curve-fit average of previous cycles as well as the average monthly values from solar cycle #23.

To download the solar flux table for use with DAS 2.0, visit: http://www.orbitaldebris.jsc.nasa.gov/mitigate/das.html

To see the latest NOAA/SEC Monthly forecast for Cycle #24, visit: http://www.swpc.noaa.gov/ftpdir/weekly/Predict.txt ♦

Geosynchronous (GEO) Environment for ORDEM2008

P. H. KRISKO

NASA's updated Orbital Debris Engineering Model (ORDEM2008) is the first of the series to include the capability of determining debris flux in the geosynchronous (GEO) region of Earth orbit. That debris population for the years 1995-2035 is restricted to sizes larger than 10 cm, which is well below the minimum cataloged object size of ~ 70 cm. Near-GEO orbital dynamics require that each object be defined further by its semi-major axis (*i.e.*, mean motion), eccentricity, inclination, and right ascension of ascending node (RAAN).

As in low Earth orbit (LEO), Space Surveillance Network (SSN) cataloged object sizes are determined by radar cross sections (RCSs) combined with the NASA Size Estimation Model (SEM). The GEO catalog includes intacts (spacecraft, upper stages, and mission-related debris), and breakup fragments. With two verified explosive breakups in the GEO region, the ratio of these cataloged objects is about 200:1, respectively. Recently, observations by telescope systems (*e.g.*, ESA's 1-meter Tenerife Telescope and NASA's Michigan Orbital Debris Survey Telescope (MODEST)) have revealed a near-GEO environment that includes a large population of dim, non-cataloged objects (*i.e.*, uncorrelated targets (UCTs)) that are presumably smaller than 70 cm. Efforts at tracking these objects to compile sets of representative orbital elements are underway.

Data available to NASA for the derivation of the GEO environment to 10 cm are the SSN catalog and MODEST survey data. Requirements are the following. First, cataloged objects must be represented correctly. Second, the dimmer (smaller) UCTs must be included with justifiable orbital elements. Third, objects that are surmised but not observed (*e.g.*, those below MODEST sensitivity of about 17 absolute magnitude or smaller than about 30 cm) must be treated reasonably. All requirements are met in ORDEM2008 by use of NASA's long-term debris evolutionary model, LEGEND, and MODEST UCT survey data (2004-2006)

continued on page 10

GEO Environment

continued from page 9

of single observations of objects which is extended to 10 cm by considering MODEST UCTs to be fragmentation debris.

LEGEND input objects are stored in standard yearly database files which include all orbital inserts, maneuvers, and breakup events from 1957 through the present. The ORDEM2008 historical GEO-cataloged environment is thus derived from 1995 to 2006. To extend this to the ORDEM2008 end date of 2035, an 8-year database cycle is applied, with statistically derived breakup events, over 100 Monte Carlo iterations. Figures 1a and 1b display the LEGEND population in 2006 in terms of mean motion vs. eccentricity and inclination vs. RAAN, respectively. The cataloged objects included in this population are those that were launched and operational into geosynchronous orbits (*i.e.*, inclination ~ 0°, eccentricity ~ 0, mean motion ~ 1 revolution/day). At satellite end-of-life or end-of-stationkeeping the dynamics of the region allows eccentricity and mean motion to remain nearly constant, as noted in the population density Figure 1a, while RAAN and inclination drift in a 53-year cycle (Figure 1b).

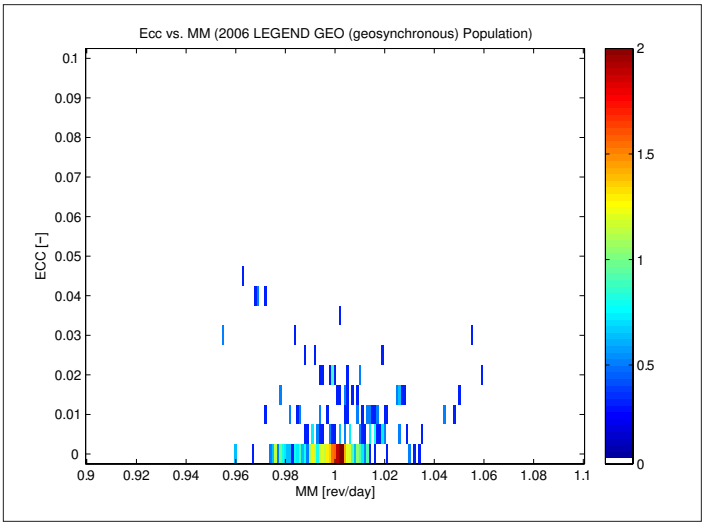

Figure 1a. LEGEND GEO population for 2006. Eccentricity vs. mean motion.

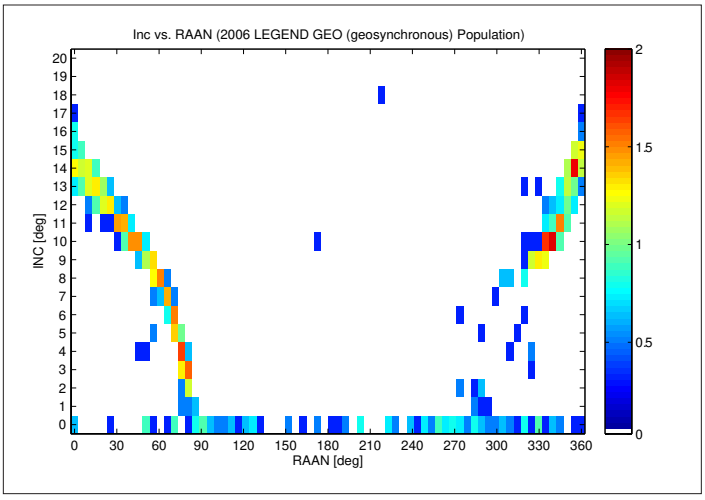

Figure 1b. LEGEND GEO population for 2006. Inclination vs. RAAN.

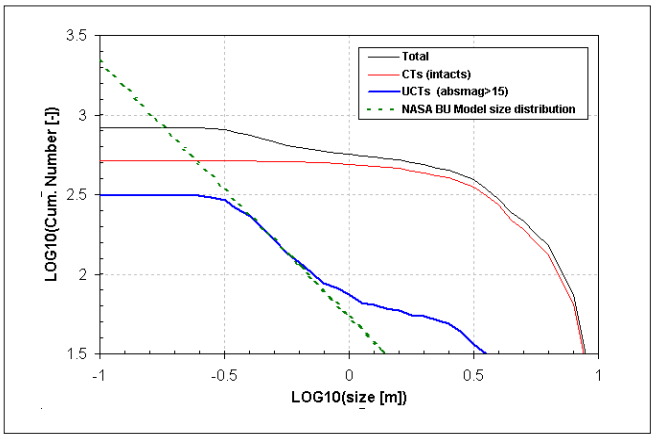

Figure 2. Cumulative size of UCTs vs. NASA Standard Breakup Model Distribution.

UCTs observed by MODEST are estimated to be larger than about 30 cm. With few geosynchronous spacecraft smaller than 1 meter, consideration of these observations as fragmentation debris appears to be reasonable. This is bolstered by the character of the UCT survey data (2004-2006) at absolute magnitudes above 15, which appears to show increasing UCT number with decreasing brightness. In Figure 2 the slope of unbiased numbers vs. estimated sizes of these UCTs is consistent with a characteristic size slope in log-log space that approximates that of the –1.6 slope for explosive fragmentation debris seen in LEO.

The single observations in MODEST measurements are those of objects moving through the telescope field-of-view at rates near GEO orbit rates at the point of observation. Therefore, survey files contain high quality inclination and RAAN measurements, but with assumed circular orbits (ACO) the eccentricity and mean motion values are not reliable. For this latter pair of elements a method of assigning more reasonable values has been developed that uses a template of fragments from 1500 randomly generated, explosive breakups in GEO over the years 1964-2006. This template, used as a probability distribution function-dependent on fragment size, assigns eccentricity and mean motion to all MODEST UCTs that are consistent with explosive breakup fragments. The fragment population extended to 10 cm, as explained above, requires eccentricity and mean motion values derived in this way as well. Additionally, inclination and RAAN are assigned based on probability density functions derived from the MODEST UCT data itself. Figures 3a and 3b illustrate the MODEST derived population density charts for presumed fragmentation debris in GEO to 10 cm. These objects, combined with those of cataloged objects in Figures 1a and 1b, form the GEO environment for ORDEM2008. ♦

figures continued on page 11

GEO Environment

continued from page 10

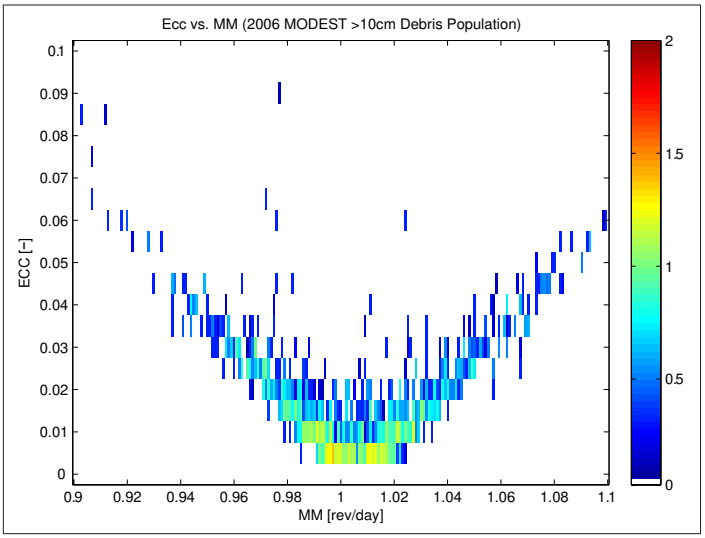

Figure 3a. Extended MODEST GEO population for 2006. Eccentricity vs. mean motion.

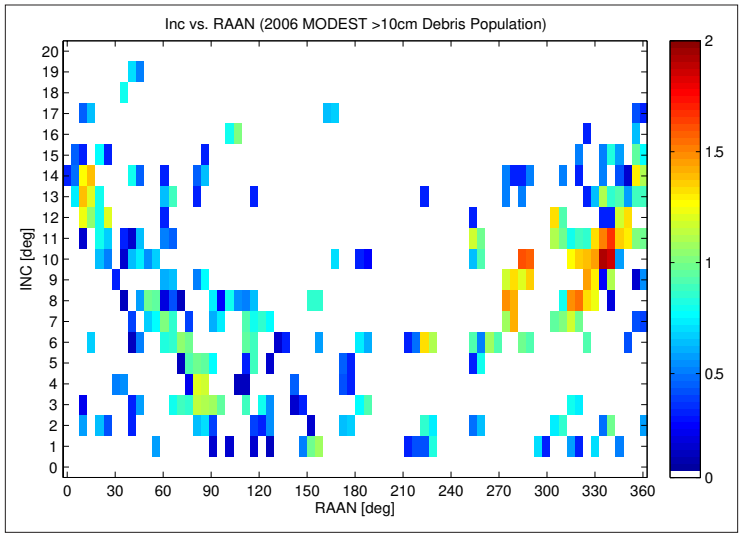

Figure 3b. Extended MODEST GEO population for 2006. Inclination vs. RAAN.

ABSTRACTS FROM THE NASA ORBITAL DEBRIS PROGRAM OFFICE

3rd IAASS Conference
21-23 October 2008, Rome, Italy

Satellite Reentry Risk Assessments at NASA

N. JOHNSON

Since 1995 NASA has required an assessment of human casualty risks arising from the reentry of every agency spacecraft, launch vehicle stage, and other large orbital objects. The NASA-originated objective, later adopted and incorporated into the U.S. Government Orbital Debris Mitigation Standard Practices and other national space debris mitigation guidelines, is to limit such human casualty risks to less than 1 in 10,000 per reentry event. By comparison, the maximum human casualty threshold for many space launch operations is a more restrictive value, *i.e.*, 0.3 in 10,000. If the anticipated design of the vehicle would result in a human casualty risk greater than 1 in 10,000, then options for long-term disposal orbits above LEO or directed de-orbits into an uninhabited broad ocean area are examined. Neither option is normally attractive due to higher vehicle energy and/or mass requirements.

NASA currently maintains two levels of reentry risk assessment software: DAS (Debris Assessment Software) for use by non-expert project personnel and the higher fidelity ORSAT (Object Reentry Survival Analysis Tool), operated by trained specialists at the NASA Johnson Space Center. Vehicles found to be compliant with human casualty risk limits by the slightly conservative DAS, need not be reevaluated by ORSAT. If, on the other hand, DAS finds a vehicle non-compliant with human casualty risks, a more detailed assessment with ORSAT is usually required. Due to the higher fidelity and greater range of evaluation options with ORSAT, some components calculated to survive by DAS might, in fact, be found to demise by ORSAT. Both software programs convert debris casualty areas into explicit casualty risks based upon the orbital inclination, year of reentry, and other factors.

Evaluations begin prior to Preliminary Design Review to identify components which are likely to survive and which might be candidates for alteration to enhance demise during reentry. To support this effort, NASA's Goddard Space Flight Center promotes a design-to-demise engineering activity. In cases where significant numbers of components might survive reentry, means to prevent them from separating from one another might be an option to reduce human casualty risks on the ground. Only debris with impacting energies greater than 15 joules are considered a significant human casualty risk.

The paper reviews examples of NASA reentry risk assessments. Safety compliance challenges to future space vehicles and components are also discussed. ♦

Statistical Issues for Uncontrolled Reentry Hazards

M MATNEY

A number of statistical tools have been developed over the years for assessing the risk of reentering object to human populations. These tools make use of the characteristics (*e.g.*, mass, shape, size) of debris that are predicted by aerothermal models to survive reentry. The statistical tools use this information to compute the probability that one or more of the surviving debris might hit a person on the ground and cause one or more casualties.

The statistical portion of the analysis relies on a number of assumptions about how the debris footprint and the human population are distributed in latitude and longitude, and how to use that information to arrive at realistic risk numbers. This inevitably involves assumptions that simplify the problem and make it tractable, but it is often difficult to test the accuracy and applicability of these assumptions.

This paper looks at a number of these theoretical assumptions, examining the mathematical basis for the hazard calculations, and outlining the conditions under which the simplifying assumptions hold. In addition, this paper will also outline some new tools for assessing ground hazard risk in useful ways.

Also, this study is able to make use of a database of known uncontrolled reentry locations measured by the United States Department of Defense. By using data from objects that were in orbit more than 30 days before reentry, sufficient time is allowed for the orbital parameters to be randomized in the way the models are designed to compute. The predicted ground footprint distributions of these objects are based on the theory that their orbits behave basically like simple Kepler orbits. However, there are a number of factors – including the effects of gravitational harmonics, the effects of the Earth's equatorial bulge on the atmosphere, and the rotation of the Earth and atmosphere – that could cause them to diverge from simple Kepler orbit behavior and change the ground footprints. The measured latitude and longitude distributions of these objects provide data that can be directly compared with the predicted distributions, providing a fundamental empirical test of the model assumptions. ♦

MEETING REPORT

3rd International Association for the Advancement of Space Safety (IAASS) Conference 21-23 October 2008, Rome, Italy

The 3rd IAASS Conference was held 21-23 October in Rome, Italy. In addition to a number of general space safety topics, there were three sessions on space traffic control and management, one on orbital debris, and four on spacecraft reentry safety. There were also a number of cross-disciplinary papers presented that were relevant to these topics, such as launch safety and the use of nuclear materials in space. Highlights included several papers on "grass roots" efforts by owners and operators of geosynchronous satellites to put together a cooperative framework for communicating detailed orbital information in an effort to avoid collisions with other operators. There were also several presentations on the recent ATV reentry over the Pacific. Also of interest were presentations on France's new comprehensive national space safety policy. During the conference gala dinner, retired NASA orbital debris scientist Don Kessler was presented with the Jerome Lederer – Space Safety Pioneer Award 2008 for his pioneering work in orbital debris science. ♦

UPCOMING MEETING

30 March - 2 April 2009: The 5th European Conference on Space Debris, ESA/ESOC, Darmstadt, Germany

The Fifth European Conference on Space Debris, through two parallel sessions, will provide a forum for presenting and discussing results and for defining future directions of research. The theme of the conference is space surveillance, with a focus on space surveillance techniques, space object catalogs, and system studies for a European space surveillance system. The conference program will also highlight all classical disciplines of space debris research. This will include radar, optical and in-situ measurements; debris environment modeling; on-orbit and re-entry risk assessments; orbit prediction and determination; debris mitigation principles; hypervelocity impacts and shielding; and standardization and policies. Abstracts should be submitted by 14 December 2008 and the deadline for papers is 29 March 2009. Additional information about the conference is available at <http://www.congrex.nl/09a03/>.

DAS 2.0 NOTICE

Attention DAS 2.0 Users: An updated solar flux table is available for use with DAS 2.0. Please go to the Orbital Debris Website (http://www.orbitaldebris.jsc.nasa.gov/mitigate/das.html) to download the updated table and subscribe for email alerts of future updates.

INTERNATIONAL SPACE MISSIONS
01 October – 31 December 2008

International Designator	Payloads	Country/ Organization	Perigee Altitude (KM)	Apogee Altitude (KM)	Inclination (DEG)	Earth Orbital Rocket Bodies	Other Cataloged Debris
2008-049A	THEOS	THAILAND	825	826	98.8	1	1
2008-050A	SOYUZ-TMA 13	RUSSIA	349	354	51.6	1	0
2008-051A	IBEX	USA	7000	220886	11.0	2	1
2008-052A	CHANDRAY AAN-1	INDIA	575	261997	18.1	1	1
2008-053A	SJ-6E	CHINA	585	602	97.7	1	1
2008-053B	SJ-6F	CHINA	582	605	97.7		
2008-054A	SKYMED 3	ITALY	621	624	97.9	1	0
2008-055A	VENESAT-1	VENEZUELA	169	41723	24.8	1	0
2008-056A	SHIYUAN 3 (SY-3)	CHINA	786.4	806.6	98.5		
2008-056B	CHUANG XIN 1-02	CHINA	786.1	807.7	98.5		
2008-057A	ASTRA 1M	LUXEM-BOURG	EN ROUTE TO GEO			1	1
2008-058A	COSMOS 2445	RUSSIA	185.5	322.0	67.2	1	0
2008-059A	STS 126	USA	343.3	351.9	51.6	0	0
2008-060A	OBJECT A	RUSSIA	349.6	358.4	51.6		
2008-061A	YAOGAN 4	CHINA	635.0	653.8	97.9		
2008-062A	COSMOS 2446	RUSSIA	650.2	39710.4	62.9	2	2
2008-063A	CIEL-2	CANADA	EN ROUTE TO GEO			1	1
2008-064A	YAOGAN 5	CHINA	489.3	496.1	97.4	1	0
2008-065A	OBJECT A	FRANCE	EN ROUTE TO GEO				
2008-065B	OBJECT B		EN ROUTE TO GEO				
2008-066A	OBJECT A	CHINA	385.1	35206.4	24.9		
2008-067A	OBJECT A	RUSSIA	19117.8	19139.2	64.8		

SATELLITE BOX SCORE
(as of 02 January 2009, as cataloged by the U.S. SPACE SURVEILLANCE NETWORK)

Country/ Organization	Payloads	Rocket Bodies & Debris	Total
CHINA	70	2704	2774
CIS	1375	3153	4528
ESA	38	36	74
FRANCE	46	330	376
INDIA	36	108	144
JAPAN	105	70	175
US	1096	3163	4259
OTHER	424	97	521
TOTAL	3190	9661	12851

Technical Editor
J.-C. Liou

Managing Editor
Debi Shoots

Correspondence concerning the ODQN can be sent to:
Debi Shoots
NASA Johnson Space Center
Orbital Debris Program Office
Mail Code JE104
Houston, TX 77058

debra.d.shoots@nasa.gov

HOW TO SUBSCRIBE...

To receive email notification when the latest newsletter is available, please fill out the ODQN Subscription Request Form located on the NASA Orbital Debris Program Office website, www.orbitaldebris.jsc.nasa.gov. This form can be accessed by clicking on "Quarterly News" in the Quick Links area of the website and selecting "ODQN Subscription" from the pop-up box that appears.

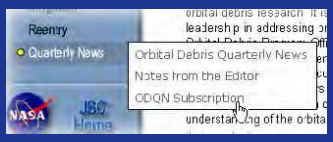

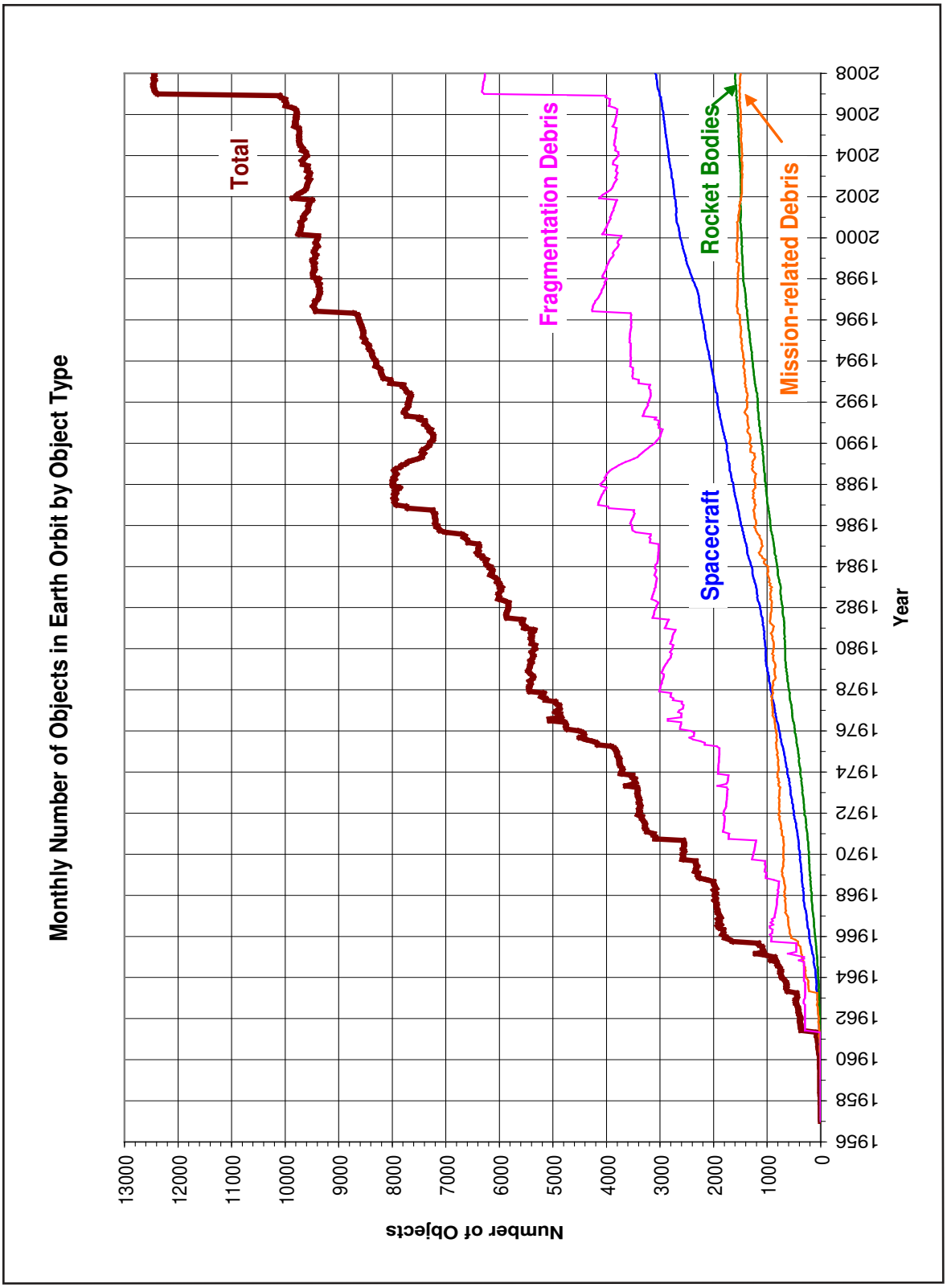

Monthly Number of Cataloged Objects in Earth Orbit by Object Type: This chart displays a summary of all objects in Earth orbit officially cataloged by the U.S. Space Surveillance Network. "Fragmentation debris" includes satellite breakup debris and anomalous event debris, while "mission-related debris" includes all objects dispensed, separated, or released as part of the planned mission.

National Aeronautics and Space Administration

Lyndon B. Johnson Space Center
2101 NASA Parkway
Houston, TX 77058

www.nasa.gov